



Universiteit  
Leiden  
The Netherlands

**NLRP3 inflammasome inhibition by the novel bispecific antibody  
InflamAb attenuates atherosclerosis in apolipoprotein e-deficient mice**

Delfos, L.; Depuydt, M.A.C.; Chemaly, M.; Coyle, S.; Schaftenaar, F.H.; Santbrink, P.J. van; ... ;  
Bot, I.

**Citation**

Delfos, L., Depuydt, M. A. C., Chemaly, M., Coyle, S., Schaftenaar, F. H., Santbrink, P. J. van, ...  
Bot, I. (2025). NLRP3 inflammasome inhibition by the novel bispecific antibody InflamAb  
attenuates atherosclerosis in apolipoprotein e-deficient mice. *Jacc: Basic To Translational  
Science*, 10(6), 826-840. doi:10.1016/j.jacbts.2024.12.012

Version: Publisher's Version  
License: [Creative Commons CC BY-NC-ND 4.0 license](#)  
Downloaded from: <https://hdl.handle.net/1887/4212171>

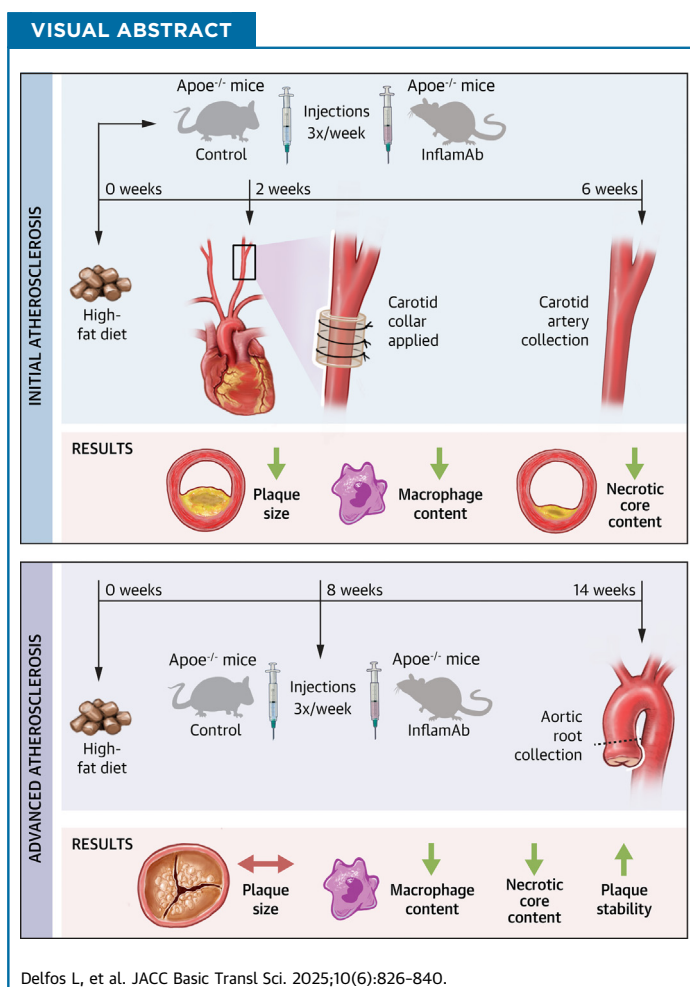
**Note:** To cite this publication please use the final published version (if applicable).

ORIGINAL RESEARCH - PRECLINICAL

# NLRP3 Inflammasome Inhibition by the Novel Bispecific Antibody InflamAb Attenuates Atherosclerosis in Apolipoprotein E-Deficient Mice



Lucie Delfos, MSc,<sup>a</sup> Marie A.C. Depuydt, PhD,<sup>a</sup> Melody Chemaly, PhD,<sup>b</sup> Sophie Coyle, MSc,<sup>b</sup> Frank H. Schaftenaar, PhD,<sup>a</sup> Peter J. van Santbrink, BSc,<sup>a</sup> Pier P. Lindenberg, MSc,<sup>a</sup> Mireia N.A. Bernabé Kleijn, BSc,<sup>a</sup> Ciara Costello, MSc,<sup>b</sup> Christine A. Power, PhD,<sup>c</sup> Rebecca Coll, PhD,<sup>d</sup> Aaron Peace, MD, PhD,<sup>e</sup> Meredith Gregory-Ksander, PhD,<sup>f</sup> Amanda C. Foks, PhD,<sup>a</sup> Johan Kuiper, PhD,<sup>a</sup> Victoria McGilligan, PhD,<sup>b,\*</sup> Ilze Bot, PhD<sup>a,\*</sup>



## HIGHLIGHTS

- We developed a novel bispecific antibody, InflamAb, designed to target the IL-1R1 for cell entrance and inhibit the intracellular NLRP3 inflammasome.
- InflamAb potently inhibits NLRP3 inflammasome-induced IL-1 $\beta$  production in vitro in BMDMs.
- InflamAb potently inhibits NLRP3 inflammasome-induced IL-1 $\beta$  production upon hyperlipidemia in vivo in *Apoe*<sup>-/-</sup> mice.
- InflamAb inhibits atherosclerotic plaque development in *Apoe*<sup>-/-</sup> mice.
- InflamAb enhances stabilization parameters of advanced plaques in *Apoe*<sup>-/-</sup> mice.

## SUMMARY

The NLRP3 inflammasome contributes to the inflammatory process in atherosclerosis by producing IL-1 $\beta$ . Components of the intracellular NLRP3 inflammasome have been shown to be expressed by macrophages in the atherosclerotic plaque and are a potential therapeutic target. We aimed to determine the efficacy of the novel bispecific antibody InflamAb, designed to target the interleukin-1 receptor type 1 and the NLRP3 inflammasome, in inhibiting atherosclerosis. InflamAb effectively inhibited IL-1 $\beta$  secretion from bone marrow-derived macrophages and reduced circulating IL-1 $\beta$  levels in vivo. Furthermore, InflamAb treatment significantly inhibited atherosclerotic plaque development, accompanied by a reduction in relative macrophage and necrotic core content. InflamAb treatment did not affect the size of established atherosclerotic lesions; however, InflamAb significantly reduced relative macrophage and necrotic core content in these plaques. To conclude, inhibition of the NLRP3 inflammasome by the bispecific antibody InflamAb shows promising efficacy in inhibiting atherosclerotic plaque development and destabilization in *ApoE*<sup>-/-</sup> mice. (JACC Basic Transl Sci. 2025;10:826-840) © 2025 The Authors. Published by Elsevier on behalf of the American College of Cardiology Foundation. This is an open access article under the CC BY-NC-ND license (<http://creativecommons.org/licenses/by-nc-nd/4.0/>).

**A**cute cardiovascular syndromes (ACS), such as myocardial infarction and stroke, remain a major cause of death worldwide. The pathologic feature giving rise to these syndromes is atherosclerosis, which is characterized by the accumulation of lipids and inflammatory cells in the large and medium-sized arteries.<sup>1,2</sup> Several immune cell subsets of both the myeloid and the lymphoid lineages have been shown to contribute to the ongoing low-grade inflammation in atherosclerosis. Macrophages are a prominent immune cell type in both human<sup>3</sup> and mouse atherosclerosis<sup>4</sup> and are derived from monocytes that infiltrate the atherosclerotic lesion.<sup>5</sup> A proportion of intraplaque macrophages may also derive from vascular proliferating macrophages.<sup>5,6</sup> In addition, smooth muscle cells have been shown to transdifferentiate and present a macrophage-like phenotype.<sup>7</sup> In atherosclerotic plaque, macrophages can produce pro- and anti-inflammatory cytokines, form foam cells by engulfing modified low-density lipoprotein (LDL), and clear apoptotic cells via efferocytosis.<sup>8,9</sup>

In recent years, several macrophage subsets have been identified, each with specific characteristics and

inflammatory functions.<sup>10</sup> Nowadays, single-cell RNA-sequencing technology has identified 3 major macrophage populations present in both human and mouse atherosclerotic vessels: resident, inflammatory, and foamy macrophages. Inflammatory macrophages largely express pro-inflammatory genes and are suggested to be derived from monocytes in the blood.<sup>4,11</sup> Within the mouse inflammatory macrophages, 2 subpopulations have been identified and classified as inflammatory *Nlrp3* and the CCR2<sup>int</sup>MHCII<sup>+</sup> macrophages. Inflammatory *Nlrp3* macrophages highly expressed *Nlrp3* and Interleukin-1 $\beta$ .<sup>11</sup>

The NLRP3 inflammasome is a multi-protein complex located inside the cell and is composed of a sensor called NLRP3 (NOD [nucleotide oligomerization domain]-, LRR [leucine-rich repeat-, and PYD [pyrin domain]-containing protein 3), an adaptor the apoptosis speck-like protein (ASC), and caspase-1, the effector. This inflammasome can be activated by a wide range of stimuli.<sup>12,13</sup> Moreover, the NLRP3 inflammasome has been described to be an important driver of atherosclerotic inflammation.<sup>13</sup> In

## ABBREVIATIONS AND ACRONYMS

<b>Alum</b>	= aluminium hydroxide
<b>ApoE<sup>-/-</sup></b>	= apolipoprotein E deficient
<b>ASC</b>	= apoptosis speck-like protein
<b>CC</b>	= cholesterol crystals
<b>DAMP</b>	= danger-associated molecular pattern
<b>ELISA</b>	= enzyme-linked immunosorbent assay
<b>IL</b>	= interleukin
<b>IL-1R1</b>	= interleukin-1 receptor type 1
<b>LDL</b>	= low-density lipoprotein
<b>LPS</b>	= lipopolysaccharides
<b>NLRP3</b>	= NOD (nucleotide oligomerization domain)-, LRR (leucine-rich repeat)-, and PYD (pyrin domain)-containing protein 3)
<b>oxLDL</b>	= oxidized LDL
<b>BMDM</b>	= bone marrow-derived macrophage
<b>PAMP</b>	= pathogen-associated molecular pattern
<b>PBS</b>	= phosphate-buffered saline
<b>PC</b>	= peritoneal cavity
<b>PRR</b>	= pattern recognition receptor
<b>TNF</b>	= tumor necrosis factor
<b>WTD</b>	= Western-type diet

From the <sup>a</sup>Division of BioTherapeutics, Leiden Academic Centre for Drug Research, Leiden University, Leiden, the Netherlands;

<sup>b</sup>Personalised Medicine Centre, School of Medicine, Ulster University, Derry-Londonderry, Northern Ireland, United Kingdom;

<sup>c</sup>Christine Power Consulting, Thoiry, Auvergne-Rhône-Alpes, France; <sup>d</sup>School of Medicine, Dentistry and Biomedical Sciences, Wellcome Wolfson Institute for Experimental Medicine; <sup>e</sup>Department of Cardiology, Western Health and Social Care Trust, Derry, United Kingdom; and the <sup>f</sup>Department of Ophthalmology, Schepens Eye Research Institute, Massachusetts Eye & Ear Infirmary and Harvard Medical School, Boston, Massachusetts, USA. \*These authors are joint senior authors.

The authors attest they are in compliance with human studies committees and animal welfare regulations of the authors' institutions and Food and Drug Administration guidelines, including patient consent where appropriate. For more information, visit the [Author Center](#).

human carotid artery plaques, NLRP3 mRNA was seen to be expressed at a higher level compared with control obtained from transplant material, and expression was higher in plaques of symptomatic versus asymptomatic patients.<sup>14</sup> NLRP3 inflammasome components are predominantly expressed in macrophages and foam cells.<sup>14,15</sup> Upon activation, the NLRP3 inflammasome contributes to the ongoing inflammatory response via activation of the inflammatory cytokines IL-1 $\beta$  and IL-18. Activation of the NLRP3 inflammasome requires a priming signal, which can occur through binding of pathogen-associated molecular patterns (PAMPs) or danger-associated molecular patterns (DAMPs) signaling to pattern recognition receptors (PRR). An alternative priming pathway is via IL-1 $\beta$  itself through IL-1 receptor type 1 (IL-1R1).<sup>12,16-18</sup> Priming results in the transcriptional upregulation of the NLRP3 inflammasome components and the pro-forms of IL-1 $\beta$  and IL-18.<sup>12,16</sup> Cholesterol crystals (CC) and oxidized LDL (oxLDL), present in both initial and advanced atherosclerosis, act as second-activation signals,<sup>19,20</sup> leading to the assembly of the NLRP3 inflammasome. Then, caspase-1, also known as interleukin-1 converting enzyme, is activated and cleaves pro-IL-1 $\beta$  and pro-IL-18 into their active forms, IL-1 $\beta$  and IL-18. Next, gasdermin D is cleaved and releases IL-1 $\beta$  and IL-18 by pore formation.<sup>12,16</sup>

In the previous, direct systemic targeting of IL-1 $\beta$  with the monoclonal antibody canakinumab significantly lowered the rate of recurrence of cardiovascular events in patients with previous myocardial infarctions. However, this coincided with a higher occurrence of fatal infections and sepsis.<sup>21</sup> Intervention in NLRP3 inflammasome activation using small-molecule MCC950 reduced atherosclerotic plaque development in vivo, which resulted from reduced macrophage content in the plaque.<sup>22</sup> However, in phase II clinical studies for rheumatoid arthritis with MCC950, a higher risk of drug-induced liver injury was found, which may be due to a high daily dose and high lipophilicity, both associated with hepatotoxicity risk.<sup>23-25</sup> To circumvent the side effects described in those studies, alternative strategies to inhibit the NLRP3 inflammasome specifically in cells that contribute to the disease process are required. Therefore, we developed a novel bispecific antibody, InflamAb, designed to target both the IL-1R1 and the NLRP3 inflammasome. Via the IL-1R1, the antibody becomes internalized, presumably by receptor-mediated endocytosis. Internalization of the bispecific antibody allows the antibody to reach the intracellular NLRP3 inflammasome target, where it can

exert its inhibitory activity. The construction of the bispecific antibody InflamAb is described elsewhere.<sup>26</sup> In this study, we aimed to determine the ability of InflamAb to inhibit atherosclerosis. First, we established the efficacy of InflamAb in vitro and in vivo, after which we assessed the therapeutic anti-atherosclerotic potential of InflamAb during the development of atherosclerosis and in more advanced plaques in *Apoe*<sup>-/-</sup> mice.

## METHODS

### GENERATION OF A BISPECIFIC ANTIBODY InflamAb, TARGETING THE IL-1R1 AND THE NLRP3 INFLAMMASOME.

The construction of InflamAb is fully described in patent application WO2020053447A1.<sup>26</sup> In brief, monoclonal antibodies targeting IL-1R1 and NLRP3 were generated at Fusion Antibodies in Northern Ireland using hybridoma technology after immunization of the mice with the respective human target proteins. After identification of functionally relevant antibodies from the hybridoma supernatants, the antibody heavy and light chain variable regions were cloned, sequenced, and reformatted onto a mouse IgG2a framework. The bispecific antibody InflamAb was generated by fusion of a scFV against NLRP3 to the C-terminal of the heavy chain of mouse IgG2a mAb. The bispecific antibody was transiently expressed in Expi-CHO cells and purified using protein A affinity chromatography at Fusion Antibodies. Because of similar peptide sequences, InflamAb also cross-reacts with the mouse proteins, which was confirmed in previous in vitro studies as part of the development process.

**HUMAN ATHEROSCLEROTIC PLAQUE SINGLE-CELL RNA SEQUENCING (scRNA-SEQ) DATA.** To determine which cell populations express both NLRP3 and IL1R1 in human atherosclerotic plaques, publicly available scRNA-seq data sets of human atherosclerotic plaque (GSE155512, GSE159677, GSE131778, GSE253903)<sup>27-30</sup> were downloaded, proximal adjacent samples were excluded from GSE159677, and the data sets were combined into a single object using Seurat packages (version 5.1.0)<sup>31</sup> in R (version 4.4.1). Filtering was performed by removing doublets cells using scDblFinder (version 1.18.0),<sup>32</sup> removing ambient RNA contamination by applying the decontX function of the celda R package (version 1.20.0),<sup>33</sup> and excluding cells with a mitochondrial gene percentage exceeding 10%, a total count of <800 or <500 unique genes detected. Layers were split based on the unique patient identifiers. The data were normalized and scaled, and variable features were identified for each

layer, using the SCTransform function of Seurat v5. Subsequently, integration was performed using the IntegrateLayers function of Seurat v5, where “RPCAIntegration” was specified in “method” argument and “SCT” was specified in the “normalization.method” argument. Double-positive cells were identified using the WhichCells function of Seurat v5. The function’s “expression” argument was set to “NLRP3 >0.5 & IL1R1 >0.5.”

**CELL CULTURE.** Bone marrow was collected by flushing femurs and tibias from C57BL/6J mice with ice-cold phosphate-buffered saline (PBS). Single-cell suspensions were obtained using a 70- $\mu$ m cell strainer. Bone marrow cells were seeded at a density of  $1/10^6$  cells/mL and differentiated into bone marrow-derived macrophages (BMDMs) by culturing for 7 days in RPMI with 10% FCS, 100 U/mL penicillin/streptomycin, 2 mM L-glutamine, and 10 ng/mL m-CSF (Immunotools). To assess the efficacy of InflamAb in vitro,  $0.1/10^6$  BMDMs/well were plated in flat-bottom 96-well plates. After adhering overnight, cells were exposed to 50 ng/mL lipopolysaccharides (LPS) (*Salmonella minnesota* R595, List Biological Laboratories Inc.) for 3 hours. After removal of the LPS, the cells were exposed to either 2.5 or 25 ng/mL InflamAb for 30 minutes. Subsequently, 50  $\mu$ g/mL aluminum hydroxide (Alum, Brenntag Biosector A/S) was added for 1 hour to activate the NLRP3 inflammasome, after which the supernatant was collected. IL-1 $\beta$  and tumor necrosis factor- $\alpha$  (TNF $\alpha$ ) concentrations were measured using mouse IL-1 $\beta$  and TNF $\alpha$  enzyme-linked immunosorbent assays (ELISAs) according to the manufacturer’s protocol (BioLegend).

To assess the efficacy of InflamAb in a human cell line in vitro, THP-1 cells (ECACC) were seeded in a 96-well plate (Sarstedt) at a density of 100,000 cells/well in complete RPMI containing 10% FBS, 1% penicillin/streptomycin, and PMA (50 ng/mL). Cells were incubated for 48 hours in PMA to allow them to differentiate. After 48 hours, the medium was replaced with complete RPMI media without PMA. Cells were then left for another 24 hours before being primed with LPS (1  $\mu$ g/mL) for 3 hours. InflamAb (50  $\mu$ g/mL) or control antibodies were added for 24 hours. Cells were then activated with Nigericin (10  $\mu$ M) (N7143, Sigma-Aldrich) for 60 minutes before supernatants were removed and stored at  $-80^{\circ}\text{C}$  until further analysis. THP-1 supernatants were diluted 1/25 before the IL-1 $\beta$  ELISA (88-7261-77, ThermoFisher) or neat for a Caspase-Glo 1 Inflammasome Assay (G9951 Promega). To assess the binding of InflamAb to NLRP3, human recombinant NLRP3 protein (Cusabio) was immobilized to a

96-well plate using coating buffer, before detection with HRP-tagged InflamAb.

**ANIMAL EXPERIMENTS.** All experimental animal work was performed in compliance with the Dutch government guidelines, the Directive 2010/63/EU of the European Parliament, and the ARRIVE guidelines. Study protocols were approved by the Ethics Committee for Animal Experiments and the Animal Welfare Body of Leiden University (project numbers 106002017887 and 10600202216361). C57BL/6J and atherosclerosis-prone apolipoprotein E-deficient (*Apoe*<sup>-/-</sup>) mice were bred in the local animal facility and kept under standard laboratory conditions. Food and water were provided ad libitum.

To assess the presence of IL-1R1<sup>+</sup>NLRP3<sup>+</sup> double-positive cells in tissues of *Apoe*<sup>-/-</sup> mice, 5- to 8-week-old male *Apoe*<sup>-/-</sup> mice were fed a Western-type diet (WTD) containing 15% cocoa butter and 0.25% cholesterol for 12 weeks. At the end of the 12 weeks, the mice were anesthetized by subcutaneous administration of ketamine (100 mg/kg) and xylazine (10 mg/kg), after which sedation was monitored by toe pinch. Peritoneal cells were obtained by flushing the peritoneal cavity (PC) with 10 mL ice-cold PBS. The mice were perfused with PBS through the left ventricle, and organs, including vascular beds, were collected.

To study the efficacy of InflamAb in vivo, female *Apoe*<sup>-/-</sup> mice were fed a WTD containing 15% cocoa butter and 0.25% cholesterol for 2 weeks, during which the mice were treated with 100  $\mu$ g InflamAb or isotype control antibody (InVivoMAb mouse IgG2a Isotype, BioXCell) in PBS, 3 times per week intraperitoneally ( $n = 3$ -4 mice per group). At the end of those 2 weeks, an inflammatory challenge was performed by the intravenous injection of low-dose LPS (50  $\mu$ g/kg), a dose that we have previously shown to be effective in inducing a potent circulating IL-1 $\beta$  response.<sup>22</sup> Plasma was collected and IL-1 $\beta$ /TNF $\alpha$  levels were measured by ELISA as already described.

To assess the effects of InflamAb on atherosclerosis development, 10- to 12-week-old female *Apoe*<sup>-/-</sup> mice were fed a WTD containing 15% cocoa butter and 0.25% cholesterol. The mice were randomly divided over the treatment groups based on body weight, age, and plasma total cholesterol levels, and treatment groups were equally distributed over the different cages. From that moment onward, mice were treated with InflamAb ( $n = 11$ ) or isotype control antibody ( $n = 14$ ) 3 times per week intraperitoneally for a total of 6 weeks. At the 2-week timepoint, collars were placed as described previously.<sup>34</sup> In short, mice were anesthetized by subcutaneous injection of ketamine

(60 mg/kg), fentanyl citrate (1.26 mg/kg), and flunixin (2 mg/kg), after which sedation was monitored by toe pinch. Access to the anterior cervical triangles was gained through a sagittal anterior neck incision and both carotid arteries were carefully dissected free from the surrounding tissue. Silastic collars (Dow Corning) were placed around both carotid arteries and fixed with 3 circumferential silk ties. Subsequently, the entry wound was closed, and the animals were returned to their cages for recovery from anesthesia. Blood was collected from the tail vein at weeks 0 and 2. At week 6, mice were anesthetized as just described, after which blood was collected via orbital bleeding. Subsequently, the mice were perfused with PBS and organs isolated.

To determine the effects of InflamAb on advanced atherosclerosis, 15- to 20-week-old male *ApoE*<sup>-/-</sup> mice were fed a WTD for 8 weeks and allocated to an experimental group as just described, after which a baseline group was sacrificed (n = 7). The remaining mice continued to be fed a WTD for another 6 weeks and at the same time were treated with 100 µg InflamAb (n = 9) or isotype control (n = 10) 3 times per week intraperitoneally. Blood was collected from the tail vein at weeks 8, 10, and 12. The mice were sacrificed at week 14 as described earlier.

**BLOOD MEASUREMENTS.** Collected blood samples were centrifuged for 10 minutes at 6,000 g at 4 °C, after which plasma was stored at -80 °C. The total plasma cholesterol levels were measured with an enzymatic colorimetric assay using Precipath standardized serum (Roche) as the internal standard. Plasma glucose was measured using an Accu-Chek Instant test (Roche).

**HISTOLOGY.** The carotid arteries and aortic roots were frozen in Tissue-Tek O.C.T. compound (Sakura) and kept at -80 °C until histologic analysis, for which 10-µm cryosections of the carotid arteries and aortic roots were prepared. For each carotid artery (n = 24; 1 artery was excluded because of thrombosis, and 1 was lost to a technical issue), collection of the sections started immediately on the proximal side of the collar, and for each slide, the sections were collected every 90 µm until the complete disappearance of the plaque. Mean plaque size, plaque size at the site of maximal stenosis, plaque volume, and necrotic areas were measured using hematoxylin and eosin staining. The necrotic area was defined as the acellular debris-rich plaque area and was measured as absolute area and relative as percentage of total plaque area. A MOMA-2 antibody (1:1000, isotype IgG2b) and biotinylated Rabbit α-Rat (1:200 vector#BA-4001) as a

secondary antibody was used to stain the macrophage content in the plaque.

Cryosections of the aortic root (n = 24; 2 excluded because of technical issues), collected every 80 µm, were histologically stained with Oil-Red-O (ORO), and 3 to 4 sections covering the 3-valve area were analyzed to measure the lipid content. The same staining as for the carotid arteries was used (MOMA-2) to measure the macrophage content in the atherosclerotic plaques. A Weigert's hematoxylin nuclei stain followed by a Sirius Red staining was performed to determine the collagen content and the necrotic core size. Histologic analyses were performed with Leica QWin or the sections were imaged using a Panoramic 250 Flash III slide scanner (3DHISTECH) and analyzed with ImageJ software. Mast cells were stained with Naphthol as-d chloroacetate esterase (Sigma-Aldrich). Resting and activated mast cells were counted directly under the microscope near the atherosclerotic plaque in the perivascular tissue of the aortic root. The FAM-FLICA Caspase-1 Assay #97 (ImmunoChemistry Technologies) was used to stain the active caspase-1 in the aortic root.<sup>35</sup> Images were obtained with the slide scanner and analyzed manually by a blinded operator.

**FLOW CYTOMETRY.** A red blood cell lysis was performed on whole blood with ACK lysis buffer to obtain a single white blood cell suspension. Aortic arches were cut into smaller pieces and incubated in a digestion mixture (collagenase I [450 U/mL], collagenase XI [250 U/mL], DNase [120 U/mL], and hyaluronidase [120 U/mL]), all Sigma-Aldrich, in PBS) for 30 minutes at 37 °C while shaking. The obtained mixture was filtered through a 70-µm cell strainer to obtain a single cell suspension. To assess the level of NLRP3<sup>+</sup>IL-1R1<sup>+</sup> double-positive cells, the aortic arches of 3 individual mice were pooled. Aortic root and PC samples were assessed per individual mouse. Next, cell suspensions were stained for specific extracellular markers with flow cytometry antibodies (Table 1) for 30 minutes. For the intracellular NLRP3 antibody staining, the corresponding samples were first incubated with fixation/permeabilization (Invitrogen) for 20 minutes and washed with permeabilization buffer (Invitrogen), after which the samples were stained with the antibody for 10 minutes. All samples were analyzed using flow cytometry on the CytoFLEX (Beckman Coulter). The obtained data were analyzed with FlowJo 10.10.0 software. One peritoneal cell sample from the control group was excluded because of technical issues.



TABLE 1 Flow Cytometry Antibodies				
Target Antigen	Fluorochrome	Supplier	Catalog No.	Working Concentration
Fc block (aCD16/32)		BioLegend	101320	1:250
Fixable viability dye	eFluor780	eBioscience	15383562	1:2000 or 1:1000
NLRP3 <sup>+</sup> IL-1R1 <sup>+</sup> double-positive cells				
Extracellular				
Ly-6C	Brilliant Violet 510	BioLegend	128033	1:500
CD11b	Pacific Blue	BioLegend	101224	1:500
I-A/I-E	Brilliant Violet 650	BioLegend	107641	1:800
F4/80	FITC	BioLegend	123108	1:400
Ly-6G	PerCP/Cyanine5.5	BioLegend	127616	1:400
CD121a (IL-1 R, type I/p80)	PE	BioLegend	113505	1:50
CD45	Alexa Fluor 700	BioLegend	103128	1:1000
Intracellular				
NLRP3 (NALP3)	APC	Miltenyi Biotec	Order no. : 130-111-397	1:50
REA control antibody (I)	APC	Miltenyi Biotec	Order no. : 130-120-709	1:50
Initial atherosclerosis				
CD11b	PE	eBioscience	12-0112-83	1:1000 or 1:400
F4/80	BV421	BioLegend	123137	1:500 or 1:400
MHC-II	eVolve 655	Thermo Fisher Scientific	86-5321-42	1:800
CD11c	FITC	BioLegend	117306	1:800
Ly6G	PerCP	BioLegend	127654	1:500
Ly6C	PE-CF594	BD Biosciences	562728	1:800
CD19	BV605	BioLegend	115539	1:500
CD4	V500	BD Horizon	560782	1:1000
CD8	AF700	BioLegend	100730	1:500
CD45	Alexa Fluor 700	Thermo Fisher Scientific	56-0451-82	1:3200
Advanced atherosclerosis				
CD4	Brilliant Violet 510	BioLegend	100559	1:1000
CD8a	Alexa Fluor 700	BioLegend	100730	1:500
CD19	Brilliant Violet 605	BioLegend	115540	1:500
CD3e	FITC	eBioscience	11-0031-85	1:500
Ly6G	PerCP	BioLegend	127654	1:500
Ly6C	PE-Dazzle 594	BioLegend	128044	1:800
NK1.1, CD161	Brilliant Violet 650	BD Horizon	564143	1:500
CD45	eFluor 450	eBioscience	48-0451-82	1:500
Cd11b	PE	BioLegend	101208	1:1000
CD11b	Brilliant Violet 605	BioLegend	101257	1:500
F4/80	FITC	BioLegend	123107	1:400
CD45	PE	BioLegend	103106	1:500
Ly6C	Brilliant Violet 510	BioLegend	128033	1:500
Ly6G	PerCP-Cy5.5	BioLegend	127616	1:400
I-A/I-E	Brilliant Violet 650	BioLegend	107641	1:800
CD11c	APC	eBioscience	17-0114-82	1:500

**RNA ISOLATION, cDNA SYNTHESIS, AND qPCR.** Left carotid arteries of the initial atherosclerosis experiment were pooled (2-4 per sample) and homogenized in guanidine thiocyanate with a tissue homogenizer, after which total RNA was extracted.<sup>36</sup> Reverse transcription of RNA was performed by M-MuLV reverse transcriptase (RevertAid, MBI Fermentas) and qPCR was performed using a 7500 fast real-time PCR system (Applied Biosystems). Primer sequences are displayed in Table 2.

**STATISTICAL ANALYSIS.** Data were analyzed using Prism 9.0 (GraphPad Software, Inc.). Data are presented using individual data points and/or the mean ± SEM for each group. Outlier tests were performed using Grubbs’ test, after which significant outliers were removed from the analysis. To check for normality a Shapiro-Wilk test was performed. Data were compared using unpaired Student’s *t*-test (2 groups) or one-way analysis of variance (>2 groups) if normally distributed and Mann-Whitney *U* test (2

**TABLE 2** Primer Sequences Used for the Quantitative Real-Time PCR Analysis, Including 3 Housekeeping Genes (36B4, Rpl27, and Rpl37)

Gene	Forward primer (3'-5')	Reverse primer (3'-5')
36B4	ctgagtacaccttcccacttactga	cgactctcttcttgctcagcttt
Rpl27	cgccaagcgatccaagatcaagtc	agctgggtccctgaacacatcctg
Rpl37	agagacgaaacactaccgggactgg	cttggttctcggtgtgtccctc
Nlrp3	cttctgcacccggactgtaact	gaaggctgtgtgtgtgggtca
IL-1R1	agggactctctctgtgtttcttcc	tccctcaagacctcaggcaacag
Caspase-1	tacctggcaggaattctggagcttc	gtcagtctctggaatgtgccatcttc
CD68	ttagctgtctctcttaaggtacag	aggaccaggccaatgatgagagg
CD86	gtagagcgggatagtaacgctga	tgcacttctatttcaggcaagca
CD206	ttagcttctctctgggctttgg	tgaggatccatcttcttggcagc
Arg1	tggcagaggtccagaagaatgg	gtgagcatccaccaaatgacac
Tlr4	ctgatcatggcactgttctctctg	ggaatgtcatcagggaattgtctgag
Mmp9	tgtatagctacctgagggtctccc	ggacacatagtggagggtgctgtc
Tlr9	ccatactgcacatctctgcggt	gcgctctgtgcctatcacacacc
CD163	cagtgcctctgtcaccttg	gatctccacagctcagacagtc
IL-8	ttgttgatgctctgatgctccatgg	gaagcttcattgcccgtggaaattc
Ccl2	ctgaagccagctctctctctc	ggtgaatgagtagcagcaggtga
IL-6	agcctggaggagggaagggtct	accgggaagacctgcacagcag
Tnf- $\alpha$	acgctcttctgtactgaactcgg	actccagctgtcctccacttg
Sting	tggcctgtctatactacattgggtac	cctgcaccactgagcattgtgtatg

groups) or Kruskal-Wallis test (>2 groups) otherwise. Probability of  $P < 0.05$  was considered statistically significant.

RESULTS

**PRESENCE OF NLRP3<sup>+</sup>IL-1R1<sup>+</sup> CELLS IN ATHEROSCLEROTIC PLAQUES.** First, we established that the cells responsive to InflamAb, IL-1R1<sup>+</sup>NLRP3<sup>+</sup> double-positive cells, are present in atherosclerotic aortic arch and aortic root tissue, as well as in the PC of *Apoe*<sup>-/-</sup> mice upon hyperlipidemia (Supplemental Figures 1A and 1B). The majority of the IL-1R1<sup>+</sup>NLRP3<sup>+</sup> double-positive cells in the atherosclerotic tissue are positive for the myeloid marker CD11b (Supplemental Figure 1C). Of these myeloid CD11b<sup>+</sup> cells, especially in the aortic root, a proportion was positive for MHCII, suggesting that these cells are antigen-presenting cells such as macrophages or dendritic cells (Supplemental Figure 1D). In addition, using existing scRNA-seq data sets, we observed that also in human atherosclerotic plaques a proportion of the myeloid cell populations co-expressed IL-1R1 and NLRP (Supplemental Figure 1E).

**InflamAb REDUCES IL-1 $\beta$  LEVELS IN VITRO AND IN VIVO UPON INFLAMMASOME ACTIVATION.** Next, we determined the efficacy of InflamAb in vitro and in vivo. The in vitro efficacy of InflamAb was evaluated in mouse bone marrow-derived macrophages. As shown in Figure 1A, both dosages of InflamAb significantly inhibited the LPS/Alum-induced IL-1 $\beta$  response, whereas TNF- $\alpha$  levels were not affected by

InflamAb treatment (Supplemental Figure 2). In vivo, the efficacy of InflamAb was studied in a hyperlipidemic environment by treating WTD-fed *Apoe*<sup>-/-</sup> mice with InflamAb and challenging the mice with LPS after 2 weeks. InflamAb significantly reduced circulating IL-1 $\beta$  levels (Figure 1B) ( $P = 0.022$  at  $t = 2$  h,  $P = 0.010$  at  $t = 4$  h), whereas the TNF- $\alpha$  levels were not affected by InflamAb treatment (Figure 1B), demonstrating the efficacy as well as the specificity of InflamAb in vivo to the IL-1 $\beta$  pathway. Similarly, InflamAb significantly inhibited LPS and Nigericin-induced IL-1 $\beta$  secretion from human THP-1 macrophages (Figure 1C), whereas an IL-1R1 antibody alone, the NLRP3 ScFv fragment and a bispecific control, consisting of an inactive IL-1R1 antibody combined with the anti-NLRP3 ScFv, did not significantly reduce IL-1 $\beta$  secretion. Similarly, InflamAb significantly inhibited LPS and Nigericin-induced caspase-1 activity in THP-1 cells, whereas the bispecific control did not (Figure 1D). Binding of InflamAb to recombinant human NLRP3 protein was confirmed as well (Figure 1E).

**InflamAb DOES NOT AFFECT CIRCULATING LEUKOCYTE POPULATIONS BUT REDUCES LEVELS OF PERITONEAL INNATE IMMUNE CELLS.** After establishing that InflamAb efficiently inhibits inflammasome activation both in vitro and in vivo, we next studied the ability of the bispecific antibody to inhibit atherosclerotic lesion development by treating *Apoe*<sup>-/-</sup> mice that were equipped with perivascular collars with InflamAb (Supplemental Figure 3A). During the study, InflamAb treatment did not affect total body weight (Supplemental Figure 3B) or total cholesterol levels (Supplemental Figure 3C). Also, total body score levels were not affected, and we did not observe any signs of infection in the control or InflamAb-treated mice. At the endpoint of the study, we measured circulating leukocyte populations, which were not affected (Figures 2A through 2E). InflamAb treatment did reduce innate immune cell populations in the PC, as illustrated by a nonsignificant lower percentage of macrophages (CD11b<sup>+</sup>F4/80<sup>+</sup>, control:  $29 \pm 2\%$  vs InflamAb:  $22 \pm 2\%$ ) (Figure 2F) ( $P = 0.05$ ) and a significantly lower percentage of dendritic cells (CD11b<sup>+</sup>CD11c<sup>+</sup>MHC-II<sup>+</sup>, control:  $1.4 \pm 0.1\%$  vs InflamAb:  $0.8 \pm 0.1\%$ ) (Figure 2G) ( $P = 0.00002$ ). Also, we observed a reduction in nonclassical myeloid cells (CD11b<sup>+</sup>Ly6C<sup>lo</sup>, control:  $0.25 \pm 0.03\%$  vs InflamAb:  $0.12 \pm 0.03\%$ ) (Figure 2H) ( $P = 0.005$ ) and Ly6C<sup>mid</sup> myeloid cells (CD11b<sup>+</sup>Ly6C<sup>mid</sup>, control:  $0.7 \pm 0.1\%$  vs InflamAb:  $0.3 \pm 0.1\%$ ) (Figure 2H) ( $P = 0.003$ ).

**InflamAb INHIBITED COLLAR-INDUCED ATHEROSCLEROTIC PLAQUE DEVELOPMENT BY REDUCING MACROPHAGE LEVELS AND NECROTIC CORE AREA.** Next, we assessed



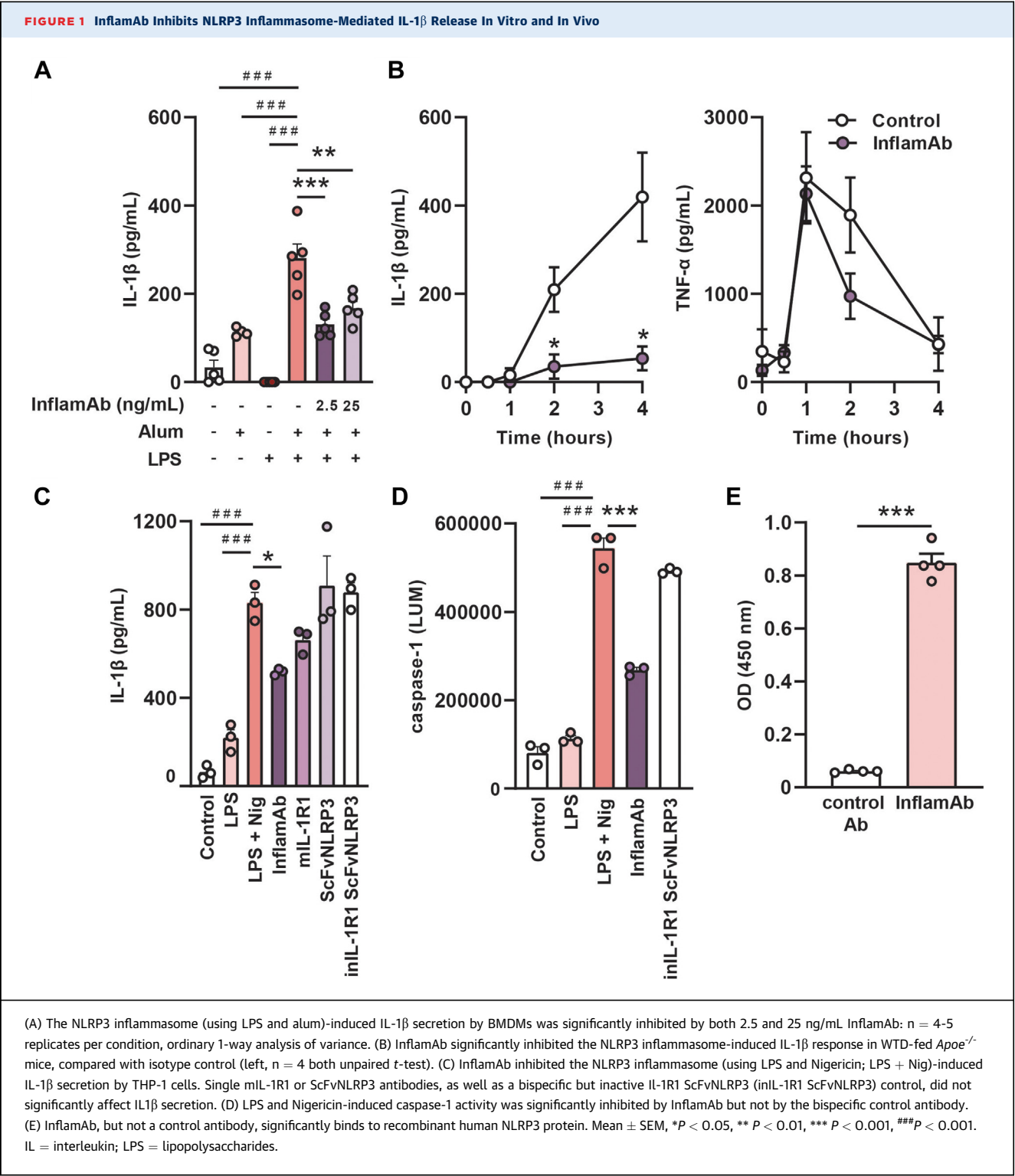
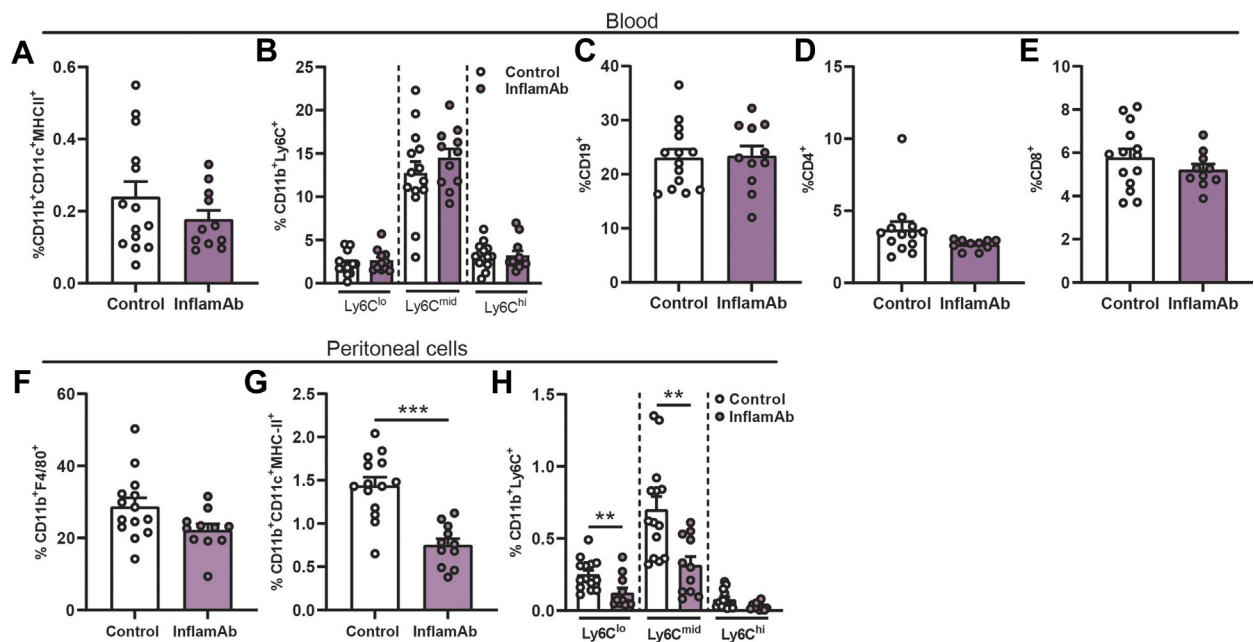


**FIGURE 2** InflamAb Treatment of *Apoe*<sup>-/-</sup> Mice Fed Western-Type Diet During Atherosclerosis Development Did Not Affect Leukocyte Populations in the Blood and Reduced Peritoneal Innate Immune Cell Populations



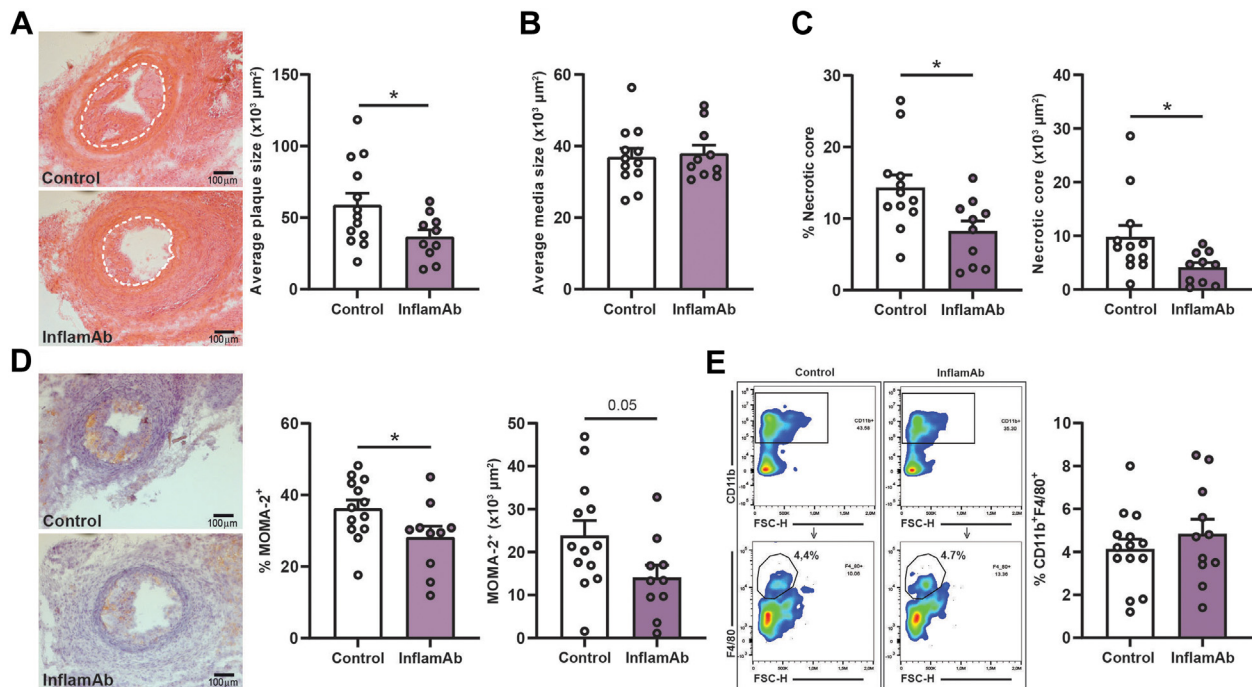
The percentage of blood (A) CD11b<sup>+</sup>CD11c<sup>+</sup>MHC-II<sup>+</sup>, (B) CD11b<sup>+</sup>Ly6C<sup>lo</sup>, CD11b<sup>+</sup>Ly6C<sup>mid</sup>, CD11b<sup>+</sup>Ly6C<sup>hi</sup>, (C) CD19<sup>+</sup>, (D) CD4<sup>+</sup>, (E) CD8<sup>+</sup> cells were not affected by InflamAb treatment. (F) The percentage of peritoneal CD11b<sup>+</sup>F4/80<sup>+</sup> cells was reduced by InflamAb compared with isotype control ( $P = 0.05$ ). (G) CD11b<sup>+</sup>CD11c<sup>+</sup>MHC-II<sup>+</sup>, (H) CD11b<sup>+</sup>Ly6C<sup>lo</sup> and CD11b<sup>+</sup>Ly6C<sup>mid</sup> peritoneal cell populations were significantly lower upon InflamAb treatment, whereas the CD11b<sup>+</sup>Ly6C<sup>hi</sup> content was not affected. (A, B) (Ly6C<sup>mid</sup>), (C, F, G, H) (Ly6C<sup>mid</sup>): control  $n = 14$ , InflamAb  $n = 11$ , unpaired  $t$ -test. (B) (Ly6C<sup>lo</sup> and Ly6C<sup>hi</sup>): control  $n = 14$ , InflamAb  $n = 11$ , Mann-Whitney test. (D) Control  $n = 13$ , InflamAb  $n = 10$ , Mann-Whitney test. (E) Control  $n = 14$ , InflamAb  $n = 10$ , unpaired  $t$ -test. (H) (Ly6C<sup>lo</sup>): control  $n = 14$ , InflamAb  $n = 11$ , Mann-Whitney test. (H) (Ly6C<sup>hi</sup>): control  $n = 13$ , InflamAb  $n = 11$ , Mann-Whitney test. All  $n$  values represent individual animals. Mean  $\pm$  SEM, all percentage of live cells, \*\* $P < 0.01$ , \*\*\* $P < 0.001$ .

carotid artery lesion size and composition. InflamAb treatment significantly inhibited atherosclerotic plaque development (control:  $59 \pm 8/10^3 \mu\text{m}^2$  versus InflamAb:  $37 \pm 5/10^3 \mu\text{m}^2$ ) (Figure 3A) ( $P = 0.043$ ), whereas InflamAb did not affect the media size (Figure 3B). Both the relative necrotic core content (control:  $14 \pm 2\%$  vs InflamAb:  $8 \pm 1\%$ ) (Figure 3C) ( $P = 0.018$ ) and the absolute necrotic core area (control:  $10 \pm 2/10^3 \mu\text{m}^2$  vs InflamAb:  $4 \pm 1/10^3 \mu\text{m}^2$ ) (Figure 3C) ( $P = 0.030$ ) were reduced upon treatment with InflamAb compared with the control group. Also, the relative macrophage content was reduced by InflamAb treatment (control:  $36 \pm 2\%$  vs InflamAb:  $28 \pm 3\%$ ) (Figure 3D) ( $P = 0.048$ ). Also, a nonsignificant lower absolute macrophage area was observed (control:  $24 \pm 4/10^3 \mu\text{m}^2$  vs InflamAb:  $14 \pm 3/10^3 \mu\text{m}^2$ ) (Figure 3D) ( $P = 0.05$ ). Macrophages as percentage of the total immune cell population in the aortic arch, as measured with flow cytometry, did not significantly differ between the 2 groups (Figure 3E). Perivascular mast cell numbers (Supplemental Figure 4A) and their activation status (Supplemental Figure 4B) were not affected by InflamAb treatment.

Similarly, as was shown previously for MMC950,<sup>22</sup> InflamAb did not affect the total mRNA expression levels of NLRP3 (Supplemental Figure 5A) or the IL-1R1 (Supplemental Figure 5B) in carotid plaques. In addition, we did not observe significant differences in genes related to macrophage phenotype or general inflammation, albeit that the expression of CD86, involved in antigen presentation and a marker of cellular activation, was almost 50% reduced (Supplemental Table 1).

**InflamAb INCREASES MARKERS OF STABILITY IN ESTABLISHED ATHEROSCLEROTIC PLAQUES BY REDUCING MACROPHAGE LEVELS AND NECROTIC CORE AREA.** In a pre-existing atherosclerosis setup (Supplemental Figure 6A), body weight (Supplemental Figure 6B), total cholesterol levels (Supplemental Figure 6C), spleen weight (Supplemental Figure 6D), and plasma glucose levels (Supplemental Figure 6E) were not affected by InflamAb. Similarly, we did not observe signs of infection in this study. At the endpoint of the study, the circulating leukocyte populations did not differ between the groups (Figures 4A to 4D). The peritoneal

**FIGURE 3** InflamAb Treatment Inhibited Collar-Induced Atherosclerotic Plaque Development in *Apoe*<sup>-/-</sup> Mice Fed Western-Type Diet



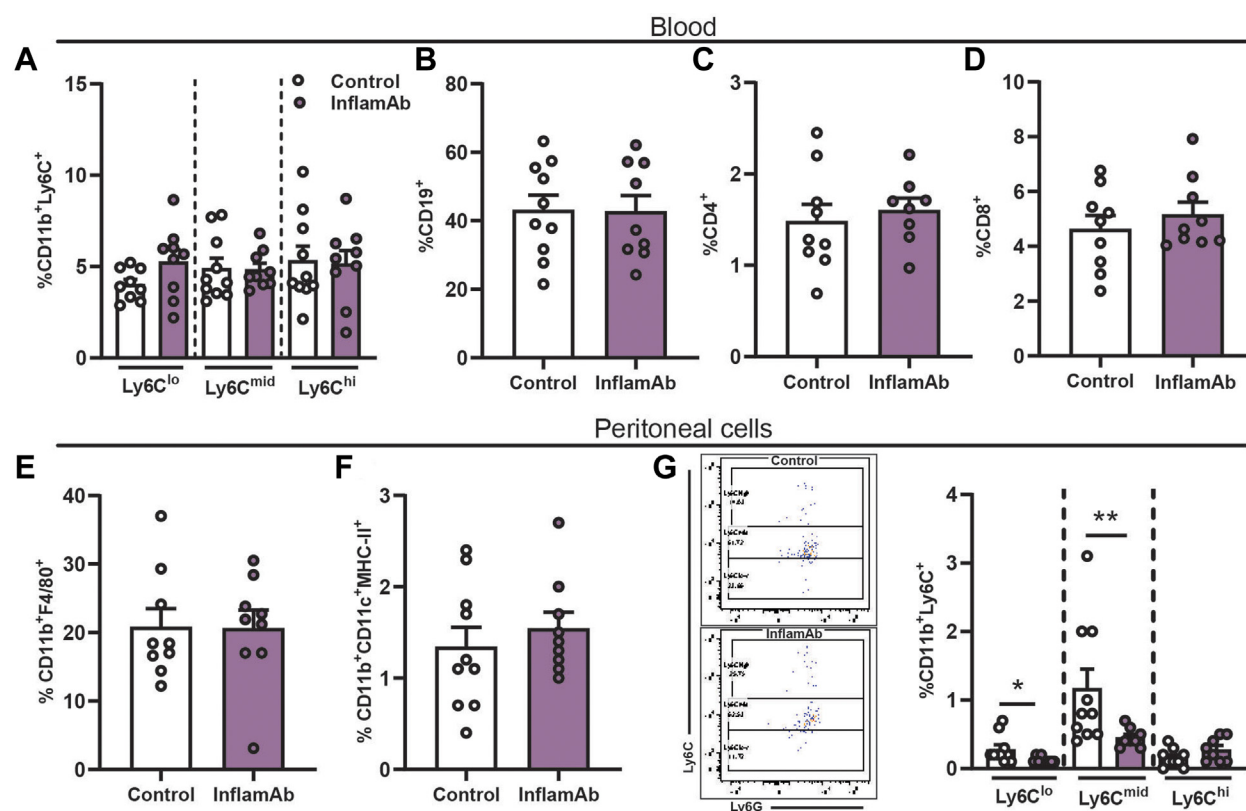
(A) Representative images of hematoxylin and eosin-stained carotid artery plaques (white dotted line = media outline, left) illustrate the reduction in average lesion size upon InflamAb treatment (right,  $n = 13$  vs  $n = 10$ , unpaired  $t$ -test). (B) The average media size was not affected ( $n = 12$  vs  $n = 10$ , unpaired  $t$ -test). (C) The relative necrotic core content ( $n = 12$  vs  $n = 10$ , unpaired  $t$ -test), and the absolute necrotic core content ( $n = 12$  vs  $n = 10$ , Mann-Whitney test) were also significantly smaller in the InflamAb treatment group than in isotype control. (D) Left, representative images of the MOMA-2<sup>+</sup> staining (red). The relative macrophage (MOMA-2<sup>+</sup>) content was shown to be significantly reduced by InflamAb. Also, a nonsignificant ( $P = 0.05$ ) lower absolute macrophage content was observed upon InflamAb treatment (both:  $n = 13$  vs  $n = 10$ , unpaired  $t$ -test). (E) Representative flow cytometry plots of CD11b<sup>+</sup> cells within the aortic CD45<sup>+</sup> population (above), followed by a F4/80<sup>+</sup> gating within this CD11b<sup>+</sup> population (below). The CD11b<sup>+</sup>F4/80<sup>+</sup> macrophage content in the aortic arch as a percentage of CD45<sup>+</sup> live cells was not affected by InflamAb ( $n = 14$  vs  $n = 11$ , unpaired  $t$ -test). All  $n$  values represent individual animals. Mean  $\pm$  SEM,  $*P < 0.05$ , scale bars = 100  $\mu$ m.

macrophage (CD11b<sup>+</sup>F4/80<sup>+</sup>) (Figure 4E) and dendritic cell (CD11b<sup>+</sup>CD11c<sup>+</sup>MHC-II<sup>+</sup>) (Figure 4F) percentages were not affected by InflamAb. However, as seen in the initial atherosclerosis study, the nonclassical myeloid cells (CD11b<sup>+</sup>Ly6C<sup>lo</sup>, control:  $0.28 \pm 0.06\%$  vs InflamAb  $0.12 \pm 0.01\%$ ) (Figure 4G) ( $P = 0.013$ ) and Ly6C<sup>mid</sup> myeloid cells (CD11b<sup>+</sup>Ly6C<sup>mid</sup>, control:  $1.17 \pm 0.28\%$  vs InflamAb:  $0.45 \pm 0.05\%$ ) (Figure 4G) ( $P = 0.008$ ) were significantly reduced by InflamAb treatment compared with the controls.

To assess the efficacy of InflamAb in this study, we measured caspase-1 activity using a Fluorescent Labeled Inhibitors of CASpases substrate, which showed significantly reduced caspase-1 activity in the InflamAb-treated mice compared with the controls (Supplemental Figure 7). InflamAb treatment of pre-existing lesions did not affect the absolute atherosclerotic plaque size and vessel occlusion parameters, measured by Oil-Red-O staining (Figure 5A). However,

these plaques displayed increased plaque stability parameters upon treatment with InflamAb, inasmuch as the relative necrotic core content was significantly reduced (control:  $21 \pm 1\%$  vs InflamAb:  $18 \pm 1\%$ ) (Figure 5B)  $P = 0.019$  Supplemental Figure 8 shows representative images of the necrotic core analysis. Collagen content, measured by Sirius Red staining, tended to be reduced upon InflamAb treatment (Figure 5B). In addition, the relative macrophage content, stained with MOMA-2<sup>+</sup>, was significantly reduced (control:  $48 \pm 2\%$  vs InflamAb:  $42 \pm 2\%$ ) (Figure 5C) ( $P = 0.031$ ). In the aortic arch, the macrophage content measured with flow cytometry did not significantly differ between the 2 groups (Figure 5D). Similarly as in the plaque development study, adventitial mast cell numbers (Supplemental Figure 9A) and activation status (Supplemental Figure 9B) in the aortic root were not affected by InflamAb treatment.

**FIGURE 4** InflamAb Treatment of Advanced Atherosclerotic Lesions in *Apoe*<sup>-/-</sup> Mice Did Not Affect Leukocyte Populations in the Blood and Reduced Myeloid Cell Population in the PC



(A) The percentage of CD11b<sup>+</sup>Ly6C<sup>lo</sup> and CD11b<sup>+</sup>Ly6C<sup>mid</sup>, (B) CD19<sup>+</sup>, (C) CD4<sup>+</sup> and (D) CD8<sup>+</sup> cells were not affected by InflamAb treatment. (E) The percentage of peritoneal CD11b<sup>+</sup>F4/80<sup>+</sup> and (F) CD11b<sup>+</sup>CD11c<sup>+</sup>MHC-II<sup>+</sup> cells did not differ between the InflamAb and control groups. (G) Representative flow charts and quantification of the CD11b<sup>+</sup>Ly6C<sup>lo</sup>, CD11b<sup>+</sup>Ly6C<sup>mid</sup> and CD11b<sup>+</sup>Ly6C<sup>hi</sup> peritoneal cells. CD11b<sup>+</sup>Ly6C<sup>lo</sup> and CD11b<sup>+</sup>Ly6C<sup>mid</sup> peritoneal cell percentages were significantly lowered by InflamAb, whereas the CD11b<sup>+</sup>Ly6C<sup>hi</sup> content was not affected. (A, E) (Ly6C<sup>lo</sup>): control n = 9, InflamAb n = 9, unpaired t-test. (A) (Ly6C<sup>mid</sup> and Ly6C<sup>hi</sup>), (B, F) control n = 10, InflamAb n = 9, unpaired t-test. (C, G) (Ly6C<sup>hi</sup>): control n = 9, InflamAb n = 8, unpaired t-test. (D) control n = 9, InflamAb n = 9, Mann-Whitney test. (G) (Ly6C<sup>lo</sup>, Ly6C<sup>mid</sup>): control n = 10, InflamAb n = 8-9, Mann-Whitney test. All n values represent individual animals. Mean ± SEM, \*P < 0.05, \*\*P < 0.01, all percentage of CD45<sup>+</sup>live cells.

## DISCUSSION

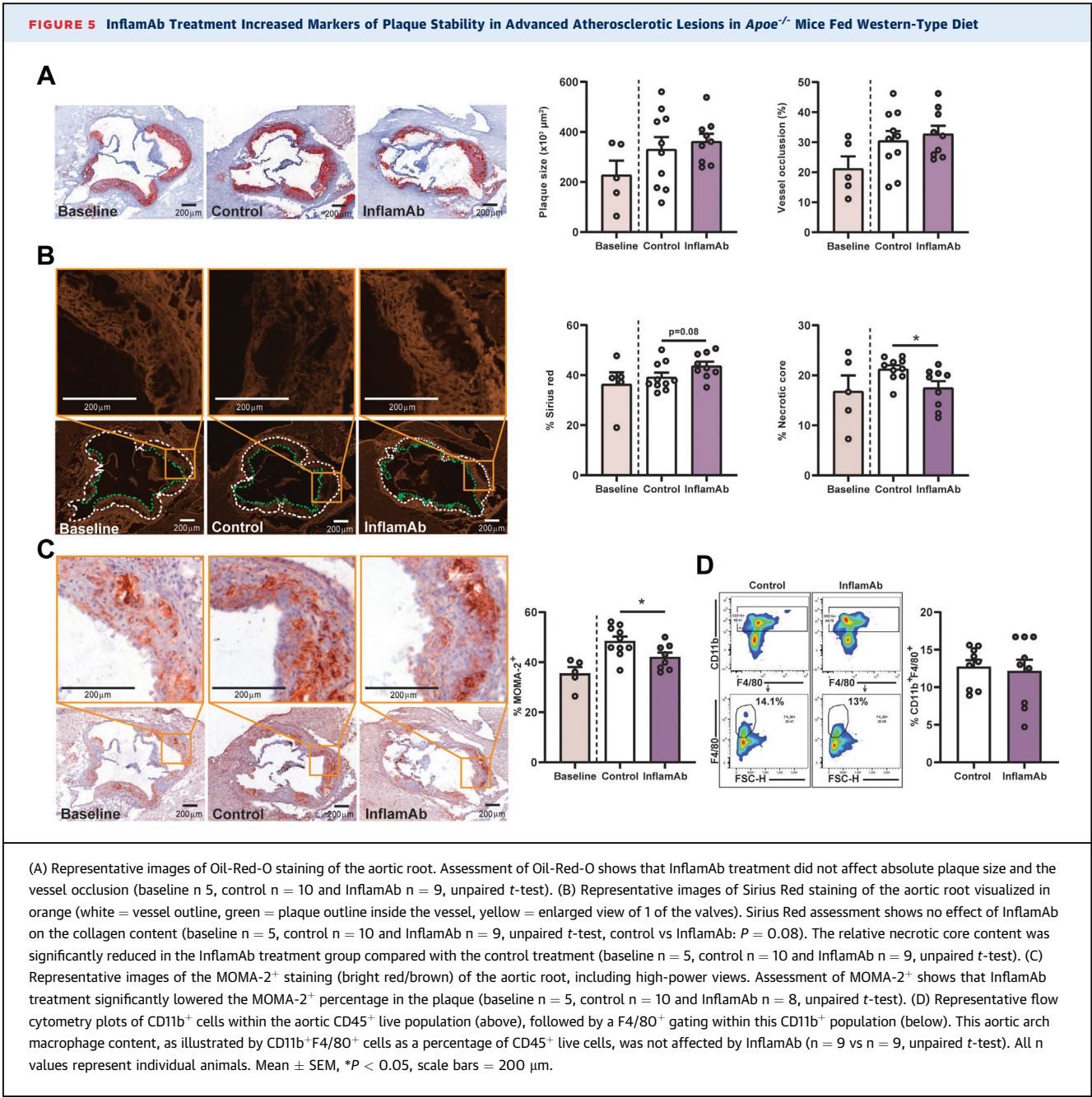
In this study, we investigated the atheroprotective efficacy of the new bispecific antibody InflamAb. The binding of the antibody to IL-1R1 acts as a ferry to deliver the bispecific antibody into the cell, and the therapeutic part (scFV) targets the intracellular NLRP3 inflammasome (Figure 6). The design of InflamAb is thus expected to result in a more specific approach than direct inhibition of IL-1 $\beta$  or targeting all NLRP3 inflammasomes with a small molecule, because InflamAb inhibits only the NLRP3 inflammasome in cells expressing the IL-1R1.

**InflamAb INHIBITS IL-1 $\beta$  SECRETION IN VITRO AND IN VIVO.** We first confirmed that NLRP3<sup>+</sup>IL-1R1<sup>+</sup> double-positive cells are present in the plaques of

hyperlipidemic *Apoe*<sup>-/-</sup> mice, confirming the suitability of the atherosclerotic mouse model, and that a subset of human plaque myeloid cells expresses both NLRP3 and IL-1R1. In these cells expressing both IL-1R1 and the NLRP3 inflammasome, IL-1 $\beta$  is able to induce its own synthesis and subsequently create an amplification loop of IL-1 $\beta$ . Moreover, we clearly establish that InflamAb potentially inhibits NLRP3 inflammasome-induced IL-1 $\beta$  production, both in vitro and upon hyperlipidemia in vivo. In addition, we were able to show that InflamAb inhibits caspase-1 activity in a subset of cells in the advanced atherosclerotic plaques, showing efficacy of InflamAb at the target site.

**InflamAb INHIBITS ATHEROSCLEROTIC PLAQUE DEVELOPMENT.** In the plaque development study,



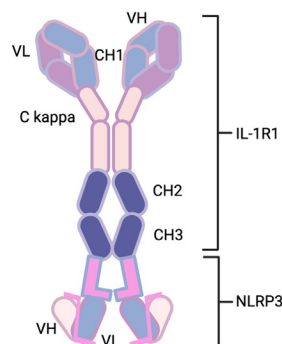


InflamAb reduced lesion size, which was caused by a reduction in both necrotic core and macrophage content. The latter finding is fully in line with our previous study, where we inhibited the NLRP3 inflammasome with the small-molecule MCC950 in this mouse model.<sup>22</sup> The reduction in intraplaque macrophages coincides with a reduction in inflammatory myeloid cells in the PC of these mice. Circulating leukocyte populations, including monocytes, were not affected by InflamAb treatment. This is in

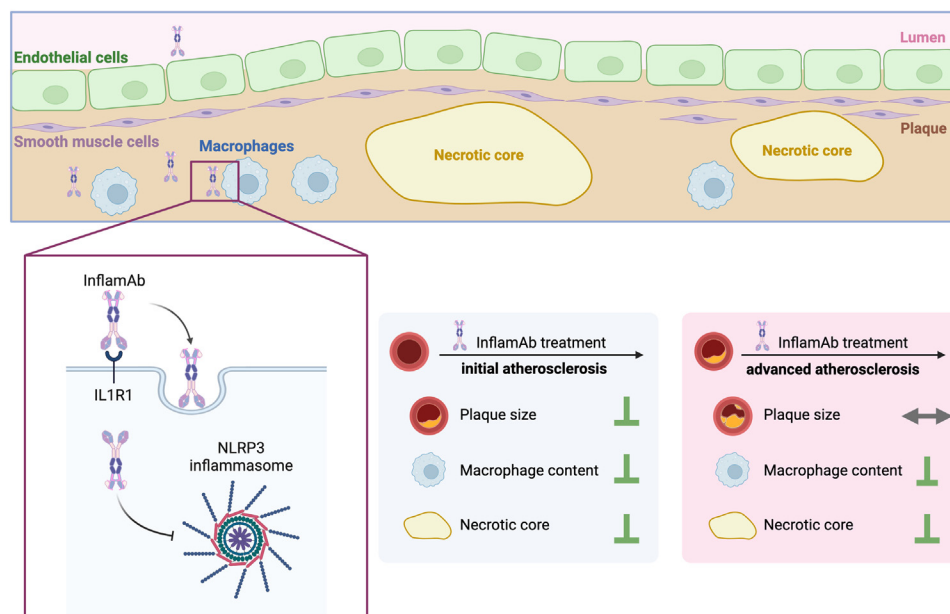
contrast with the results of a study by Hettwer et al,<sup>37</sup> who showed that inhibition of the NLRP3 inflammasome with MCC950 or treatment with an IL-1β neutralizing antibody lowered leukocyte numbers in both the circulation and atherosclerotic aortas. These findings thus illustrate a more specific and local nature of our approach. InflamAb treatment did not affect the local mRNA expression of NLRP3 and IL-1R1 in the atherosclerotic plaque, which is in line with our previous study, where MCC950 did not affect the

**FIGURE 6** Visual Summary of the InflamAb Studies

### InflamAb structure



### InflamAb inhibits atherosclerosis in apolipoprotein E-deficient mice



Visual summary of the InflamAb structure and study outcomes. Created in BioRender. Chemaly, M. (2025). <https://BioRender.com/x25m415>.

mRNA expression of NLRP3 and NLRP3-related genes in carotid artery plaques. It remains to be investigated whether the observed reduction in plaque macrophages is directly caused by a reduction in local IL-1 $\beta$  levels or via reduced adhesion and subsequent influx of immune cells. IL-1 $\beta$  deficiency in *Apoe*<sup>-/-</sup> mice, for example, resulted in decreased vascular cell adhesion molecule (VCAM)-1 and monocyte chemoattractant protein-1 (MCP-1) mRNA expression in the aorta compared with mice with IL-1 $\beta$ .<sup>38</sup> Also, in our MCC950 study, NLRP3 inflammasome inhibition led to reduced VCAM-1 and ICAM-1 mRNA expression in the carotid artery.<sup>22</sup> Similarly, Hettwer et al<sup>37</sup> showed that treatment with MCC950 reduced endothelial expression of adhesion molecules and chemoattractants in atherosclerotic aortas of *Apoe*<sup>-/-</sup> mice. Together, these findings may underlie the reduced accumulation of leukocytes, including macrophages, upon inflammasome inhibition in atherosclerosis.<sup>37</sup>

**InflamAb INCREASED PLAQUE STABILITY MARKERS IN PRE-EXISTING LESIONS.** InflamAb treatment of pre-existing lesions increased the plaque stability markers, illustrated both by a reduced macrophage and necrotic core content and by a trend toward

increased collagen content. Similarly as in the initiation study, peritoneal myeloid populations were reduced upon InflamAb treatment. During atherosclerotic lesion progression, macrophages differentiate into foam cells after uptake of oxidized or aggregated LDL. These foam cells undergo apoptosis or necrosis, thereby contributing to necrotic core formation, which enhances the probability for the lesion to rupture.<sup>2</sup> Furthermore, macrophages are known to contribute to the destabilization of plaques via the production of proteases that degrade collagen.<sup>2</sup> By limiting the macrophage accumulation, InflamAb treatment may limit necrotic core formation while also reducing degradation of extracellular matrix molecules such as collagen. Additionally, it has been shown that IL-1 $\beta$  itself increases the production of matrix metalloproteinase -1, -8, and -13 in monocytes and macrophages.<sup>39</sup> Thus, a reduction in local IL-1 $\beta$  levels in the plaque can affect the collagen content via reduced production of matrix metalloproteinase. In line with these and our findings, increased plaque stability was also observed in the study by Zheng et al<sup>40</sup> in which the NLRP3 gene was silenced using a lentiviral vector in *Apoe*<sup>-/-</sup> mice. NLRP3 silencing reduced the progression of the



plaques, and the plaques were less macrophage-rich and contained more collagen and smooth muscle cells.

**STUDY LIMITATIONS.** Here, we studied the efficacy of a novel bispecific antibody InflamAb in inhibiting plaque development and progression in a preclinical mouse model of atherosclerosis. The cellular trafficking of InflamAb via the IL-1R1 leading to intracellular NLRP3 inflammasome inhibition, however, remains to be visualized in vivo. In addition, detailed studies on cellular migration have not been performed to this date, to our knowledge. Such studies would provide more mechanistic insights in the local, but also potential systemic mechanisms involved, which now remain to be elucidated. For example, it is unknown whether InflamAb prevents active recruitment of myeloid cells to the plaque or whether InflamAb may have affected other inflammatory pathways as well, which we were unable to detect in our studies. Furthermore, although we observed promising in vitro effects of InflamAb using human cells, studies using a more humanized disease model need to be performed to further establish the translational value of our findings.

## CONCLUSIONS

The novel bispecific anti-NLRP3 antibody InflamAb inhibits plaque development and led to an increase in markers of plaque stability in more advanced plaques (Figure 6). The current encouraging data warrant further development of this therapeutic strategy against atherosclerosis and ACS.

## FUNDING SUPPORT AND AUTHOR DISCLOSURES

This work was supported by The Dutch Heart Foundation [CVON2017-20: Generating the best evidence based pharmaceutical targets and drugs for atherosclerosis (GENIUS II) to Dr Depuydt, Dr Kuiper, and Dr Bot; 2019T067 to Dr Bot (Established Investigator), 2018T051 to Dr Foks; and by the Ulster University Proof of Principle Award. All other authors have reported that they have no relationships relevant to the contents of this paper to disclose.

**ADDRESS FOR CORRESPONDENCE:** Dr Ilze Bot, Division of BioTherapeutics, Leiden Academic Center for Drug Research, Leiden University, Einsteinweg 55, 2333 CC Leiden, the Netherlands. E-mail: [i.bot@lacr.leidenuniv.nl](mailto:i.bot@lacr.leidenuniv.nl).

## PERSPECTIVES

**COMPETENCY IN MEDICAL KNOWLEDGE:** Acute cardiovascular syndromes are a leading cause of death worldwide and are generally caused by rupture or erosion of an atherosclerotic plaque. Recent studies have established that inhibition of the IL-1 $\beta$  pathway is a powerful therapeutic approach to limit the incidence of acute cardiovascular events. Here, we provide a novel tool to intervene in NLRP3 inflammasome-induced IL-1 $\beta$  production by means of the bispecific antibody InflamAb. In this study, we conclusively demonstrate that treatment of *Apoe*<sup>-/-</sup> mice with InflamAb inhibits atherosclerotic lesion development and improves the stability of more advanced plaques, rendering InflamAb a promising therapeutic lead for plaque stabilization.

**TRANSLATIONAL OUTLOOK:** From a translational perspective, the increased stability upon InflamAb treatment of pre-existing atherosclerosis is a promising finding in relation to patients with established atherosclerosis. In the CANTOS trial, where patients with previous myocardial infarctions and thus established atherosclerotic lesions were treated with an anti-IL-1 $\beta$  antibody, the potential of targeting this inflammatory pathway to limit secondary cardiovascular events was already demonstrated. Because of the systemic nature of this approach, serious side effects related to sepsis and deaths due to infection occurred, rendering a more targeted therapy necessary.<sup>21</sup> Owing to its bispecific approach to NLRP3<sup>+</sup>IL-1R1<sup>+</sup> double-positive cells, InflamAb may overcome these adverse effects, at the same time limiting plaque instability parameters. Our preclinical experiments are the first steps toward a clinical application of InflamAb against acute cardiovascular syndromes.

## REFERENCES

1. Libby P. The changing landscape of atherosclerosis. *Nature*. 2021;592:524-533.
2. Bjorkegren J, Lusis AJ. Atherosclerosis: recent developments. *Cell*. 2022;185:1630-1645.
3. Fernandez D, Rahmami AH, Fernandez NF, et al. Single-cell immune landscape of human atherosclerotic plaques. *Nat Med*. 2019;25:1576-1588.
4. Zernecke A, Winkels H, Cochain C, et al. Meta-analysis of leukocyte diversity in atherosclerotic mouse aortas. *Circ Res*. 2020;127:402-426.
5. Robbins C, Hilgendorf I, Weber GF, et al. Local proliferation dominates lesional macrophage accumulation in atherosclerosis. *Nat Med*. 2013;19:1166-1172.
6. Ensan S, Li A, Besla R, et al. Self-renewing resident arterial macrophages arise from embryonic CX3CR1<sup>+</sup> precursors and circulating monocytes immediately after birth. *Nat Immunol*. 2016;17:159-168.
7. Feil S, Fehrenbacher B, Lukowski R, et al. Transdifferentiation of vascular smooth muscle cells to macrophage-like cells during atherogenesis. *Circ Res*. 2014;115:662-667.
8. Cochain C, Zernecke A. Macrophages in vascular inflammation and atherosclerosis. *PLoS Arch*. 2017;469:485-499.
9. Cybulsky M, Cheong C, Robbins CS. Macrophages and dendritic cells partners in atherogenesis. *Circ Res*. 2016;118:637-652.
10. Wieland E, Kempen LJAP, Donners MMPC, Biessen EAL, Goossens P. Macrophage

heterogeneity in atherosclerosis: a matter of context. *Eur J Immunol*. 2024;54(1):e2350464.

11. Zernecke A, Erhard F, Weinberger T, et al. Integrated single-cell analysis-based classification of vascular mononuclear phagocytes in mouse and human atherosclerosis. *Cardiovasc Res*. 2023;119:1676-1689.

12. Swanson K, Deng M, Ting JP-Y. The NLRP3 inflammasome: molecular activation and regulation to therapeutics. *Nat Rev Immunol*. 2019;19:477-489.

13. Grebe A, Hos F, Latz E. NLRP3 inflammasome and the IL-1 pathway in atherosclerosis. *Circ Res*. 2018;122:1722-1740.

14. Varghese G, Folkersen L, Strawbridge RJ, et al. NLRP3 Inflammasome expression and activation in human atherosclerosis. *J Am Heart Assoc*. 2016;5:1-11.

15. Shi X, Xie W-L, Kong W-W, Chen D, Qu P. Expression of the NLRP3 inflammasome in carotid atherosclerosis. *J Stroke Cerebrovasc Dis*. 2015;24:2455-2466.

16. Silvius M, Demkes EJ, Fiolet ATL, et al. Immunomodulation of the NLRP3 inflammasome in atherosclerosis, coronary artery disease, and acute myocardial infarction. *J Cardiovasc Transl Res*. 2021;14:23-34.

17. Libby P. Interleukin-1 beta as a target for atherosclerosis therapy. *J Am Coll Cardiol*. 2017;70:2278-2289.

18. Dinarello C, Ikejima T, Warner SJC, et al. Interleukin 1 induces interleukin 1. I. Induction of circulating interleukin 1 in rabbits in vivo and in human mononuclear cells in vitro. *J Immunol*. 1987;139:1902-1910.

19. Duewell P, Kono H, Rayner KJ, et al. NLRP3 inflammasomes are required for atherogenesis and activated by cholesterol crystals. *Nature*. 2010;464:1357-1361.

20. Sheedy F, Grebe A, Rayner KJ, et al. CD36 coordinates NLRP3 inflammasome activation by facilitating intracellular nucleation of soluble ligands into particulate ligands in sterile inflammation. *Nature Immunol*. 2013;14:812-820.

21. Ridker P, Everett BM, Thuren T, et al. Antiinflammatory therapy with canakinumab for

atherosclerotic disease. *N Engl J Med*. 2017;377:1119-1131.

22. van der Heijden T, Kritikou E, Venema W, et al. NLRP3 Inflammasome inhibition by MCC950 reduces atherosclerotic lesion development in apolipoprotein E-deficient mice—brief report. *Arterioscler Thromb Vasc Biol*. 2017;37:1457-1461.

23. Duan M, Sun L, He X, Wang Z, Hou Y, Zhao Y. Medicinal chemistry strategies targeting NLRP3 inflammasome pathway: a recent update from 2019 to mid-2023. *Eur J Med Chem*. 2023;260:115750.

24. Shah F, Leung L, Barton HA, et al. Setting clinical exposure levels of concern for drug-induced liver injury (DILI) using mechanistic in vitro assays. *Toxicol Sci*. 2015;147:500-514.

25. Chen M, Borlak J, Tong W. High lipophilicity and high daily dose of oral medications are associated with significant risk for drug-induced liver injury. *Hepatology*. 2013;58:388-396.

26. McGilligan V, inventor. Bispecific antibody targeting IL-1R1 and NLRP3. *GB patent application PCT/EP2019/074745*. 2020.

27. Wirka RC, Wagh D, Paik DT, et al. Atheroprotective roles of smooth muscle cell phenotypic modulation and the TCF21 disease gene as revealed by single-cell analysis. *Nat Med*. 2019;25:1280-1289.

28. Pan H, Xue C, Auerbach BJ, et al. Single-cell genomics reveals a novel cell state during smooth muscle cell phenotypic switching and potential therapeutic targets for atherosclerosis in mouse and human. *Circulation*. 2020;142:2060-2075.

29. Alsaigh T, Evans D, Frankel D, Torkamani A. Decoding the transcriptome of calcified atherosclerotic plaque at single-cell resolution. *Commun Biol*. 2022;5:1084.

30. Bashore AC, Yan H, Xue C, et al. High-dimensional single-cell multimodal landscape of human carotid atherosclerosis. *Arterioscler Thromb Vasc Biol*. 2024;44:930-945.

31. Hao Y, Stuart T, Kowalski MH, et al. Dictionary learning for integrative, multimodal and scalable single-cell analysis. *Nat Biotechnol*. 2024;42:293-304.

32. Germain P-L, Lun A, Meixide CG, Macnair W, Robinson MD. Doublet identification in single-cell sequencing data using scDbtFinder. *F1000Res*. 2022;10:979.

33. Yin Y, Yajima M, Campbell J. decontX: Decontamination of single cell genomics data. Version 1.2.0. 2024. Accessed October 1, 2024. <https://www.bioconductor.org/packages/release/bioc/html/decontX.html>

34. von der Thüsen J, van Berkel TJC, Biessen EAL. Induction of rapid atherogenesis by perivascular carotid collar placement in apolipoprotein E-deficient and low-density lipoprotein receptor-deficient mice. *Circulation*. 2001;103:1164-1170.

35. Peikert A, König S, Suchanek D, et al. P2X4 deficiency reduces atherosclerosis and plaque inflammation in mice. *Sci Rep*. 2022;12:2801.

36. Chomczynski P, Sacchi N. Single-step method of RNA isolation by acid guanidinium thiocyanate-phenol-chloroform extraction. *Anal Biochem*. 1987;162:156-159.

37. Hettwer J, Hinterdobler J, Miritsch B, et al. Interleukin-1b suppression dampens inflammatory leucocyte production and uptake in atherosclerosis. *Cardiovasc Res*. 2022;118:2778-2791.

38. Kirii H, Niwa T, Yamada Y, et al. Lack of interleukin-1 $\beta$  decreases the severity of atherosclerosis in apoE-deficient mice. *Arterioscler Thromb Vasc Biol*. 2003;23:656-660.

39. Libby P. Interleukin-1 beta as a target for atherosclerosis therapy: biological basis of CANTOS and beyond. *J Am Coll Cardiol*. 2017;70:2278-2289.

40. Zheng F, Xing S, Gong Z, Mu W, Xing Q. Silence of NLRP3 suppresses atherosclerosis and stabilizes plaques in apolipoprotein E-deficient mice. *Mediators Inflamm*. 2014:1-8.

---

**KEY WORDS** atherosclerosis, bispecific antibody, interleukin-1 receptor type 1, interleukin-1 $\beta$ , NLRP3 inflammasome

---

**APPENDIX** For supplemental figures and a table, please see the online version of this paper.